Methodology of Macromodeling Demonstrated on Force Feedback Σ/Δ-Architectures

M. Handtmann[+*#], R. Aigner[+], R. Nadal[+], G. Wachutka[*]

[+]Infineon Technologies, Otto-Hahn-Ring 6, D-81730 Munich, Germany,
[#]martinh.handtmann.ext@infineon.com
[*]Institute for Physics of Electrotechnology, Munich University of Technology
Arcisstr. 21, D-80290 Munich, Germany

ABSTRACT

Design and verification of complete microsystems require effective models of the micromechanical components for the simulation at system level. Particularly for force feedback Σ/Δ-architectures, long transient simulations are inevitable to characterize the system-inherent signal processing. In this paper we present an energy-based methodology describing a general approach to deriving marcomodels of flexible, squeeze-film damped, multi-electrode structures for use in a network simulator. The coupling scheme between the kinematics of the mechanical structure and the electrical field between the electrodes allows to incorporate additional interactions such as squeeze-film damping. The flexibility of our modeling method proves to be particularly valuable for the analysis of mechanically damped eigenmodes. Complete macromodels can be extracted from fully meshed FEM and BEM model data.

1 INTRODUCTION

Micromechanical sensing applications evolve from simple one-dimensional towards complex multi-dimensional systems. State-of-the-art designs include sophisticated 3D acceleration sensors [1] or 2-axis gyroscopes [2]. As a consequence, multiple force feedback loops as system architectures are very popular. Since the feedback makes the system operate around a predefined fixed state, these architectures provide good linearisation, low cross-coupling and low sensitivity to mechanical and geometrical design parameters. They are often implemented as Σ/Δ-architectures [1]. Besides an A/D-conversion, this type of feedback architecture is favored for its perfect compatibility with integrated CMOS switched capacitor circuitry.

A quantized feedback signal is a characteristic of Σ/Δ-architectures, causing the mechanical structure to be subjected to forces which have a broadband frequency spectrum. As a vital part of the loop, the structure acts as a low-pass filter on this spectrum. Hence, parasitic excitation of a number of eigenmodes can affect the loop's stability and signal processing. Therefore, design and verification of force feedback Σ/Δ-architectures require simulation models of the micromechanical components which properly describe their dynamic behavior including the eigenmodes which lie in the frequency band of interest. These models have to be computationally efficient, since long transient simulations at system level are inevitable for the analysis of the system performance. Non-linear behavior and cross-coupling effects can additionally affect the system and should be considered within the models.

In this paper, we describe an energy-based methodology of macromodeling which is particularly suited to meet the above requirements. Established methods exist for suspended, rigid, multi-dimensional structures [3]. With a view to automated model generation, the described method is a general approach for deriving marcomodels of flexible, squeeze-film damped, multi-electrode structures for use in a network simulator. It is based on a formulation of the structure's dynamics by Lagrange's equations [4] in combination with a reduced version of Reynold's equations [5].

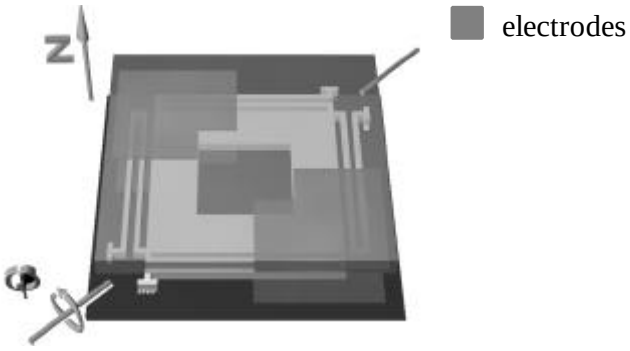

Figure 1: hinged micromechanical teststructure

The methodology is applied to a micromechanical plate, suspended on 4 springs as shown in Fig. 1. It is a teststructure for a detection and force feedback circuit, which simultaneously senses the deflection of the plate along the z-axis and the tilt around the φ-axis. Therefore, we find two electrodes on each side of the plate which, besides capacitive sensing of the position, are used for electrostatic force feedback. The plate is encapsulated between a substrate and a lid, thus forming two small gaps, which give rise to squeeze film damping.

2 THEORY

The method is based on Lagrangian equations [6]:

$$\frac{d}{dt}\left(\frac{\partial T}{\partial \dot{q}_v}\right) - \frac{\partial T}{\partial q_v} + \frac{\partial E_{pot}}{\partial q_v} = F_v$$

where T denotes the kinetic energy, E_{pot} the potential energy, q_v the generalized coordinates, $\dot{q}_v$ the generalized velocities, t the time and F_v the generalized forces.

In this approach, the kinetic energy T and the mechanical deformation energy $E_{pot,def}$ represent the kinematics of the mechanical structure. Coupling of the kinematics with conservative energy domains can be described using the potential energy [4], while the use of the generalized forces F_v allows for the coupling with non-conservative energy domains.

The Lagrange's equations contain implicitly a reduced formulation of the kinetic differential equations of the structure. A set of discrete generalized coordinates q_v has to be associated with the possible motions of the mechanical structure. For a continuously deformable structure an infinite number of coordinates would be necessary which represent the infinite number of dynamical degrees of freedoms. Hence, reduction to a limited number of coordinates restricts the possible configurations (e.g. shape and position) of the mechanical structure.

With a view to automated model generation, a basis set of orthogonal deformation shapes u_i is used to define the restricted configuration space of the structure. The generalized variables q_v are introduced as the respective linear expansion coefficients. As a consequence, the construction of the macromodel, (i.e.: the formulation of the kinetic energy T and mechanical deformation energy $E_{pot,def}$) can be easily related to data and quantities from FEM models:

$$\frac{d}{dt}\left(\frac{\partial T}{\partial \dot{q}_v}\right) = \underline{\mathbf{U}}^T \underline{\mathbf{M}}\underline{\mathbf{U}}[0 \cdots 0 \quad \ddot{q}_v \quad 0 \cdots 0]^T;\ \underline{\mathbf{U}}^T \underline{\mathbf{M}}\underline{\mathbf{U}} = \underline{\mathbf{M}_{\mathbf{red}}}$$

$$\frac{\partial E_{pot}}{\partial q_v} = \underline{\mathbf{U}}^T \underline{\mathbf{K}}\underline{\mathbf{U}}[0 \cdots 0 \quad q_v \quad 0 \cdots 0]^T;\ \underline{\mathbf{U}}^T \underline{\mathbf{K}}\underline{\mathbf{U}} = \underline{\mathbf{K}_{\mathbf{red}}}$$

Here, $\underline{\mathbf{M}}$ denotes the mass and $\underline{\mathbf{K}}$ the stiffness matrices of the FEM model, $\underline{\mathbf{U}}$ the orthonormal basis of deformation shapes with respect to the FEM model, and $\underline{\mathbf{M}_{\mathbf{red}}}$ and $\underline{\mathbf{K}_{\mathbf{red}}}$ the mass and stiffness matrices of the reduced model.

Non-linear material effects can be incorporated in the macromodel by introducing stiffness and reduced stiffness matrices which depend on the generalized coordinates q_v. Evaluation of the stiffness matrices at a number of points in the configuration space with subsequent interpolation leads to analytical expressions of the reduced stiffness matrices and of the deformation energy calculated from it. In this way, we arrive at a computational efficient macromodel.

As the energy of quasistatic electrical fields is conservative, the coupling of the mechanical and the electrical energy domain can be described by the electrical potential energy [4,8] and its derivatives, respectively:

$$\frac{\partial E_{pot,el}}{\partial q_v} = F_E = \frac{1}{2} V^T \frac{\partial [C_{ij}]}{\partial q_v} V$$

Here, C_{ij} denotes the capacitance matrix of the multi-electrode structure and V is a column vector consisting of the bias voltages on the electrodes. Since the expression requires the partial derivative of the capacitance matrix C_{ij}, an analytical expression of the matrix is desirable. Similarly to the non-linear stiffness matrix, this can be achieved by fitting BEM capacitance data of the multi-electrode system at a number of points in the considered configuration space. Furthermore, this formulation enables the implementation of the model in an electrical circuit simulator, since the applied voltages together with corresponding current terms [7] define "across" and "through" quantities, as they are required for the generalized Kirchhoffian network description.

The presented methodology also covers compressible isothermal squeeze film damping. This type of damping occurs in a thin viscous gas film in a small gap between mechanically movable parts, a situation which is very common in surface-micromachined devices. Squeeze film damping is described by Reynold's equation [9] below, in which the pressure p is substituted for the gas density r under the assumption of an isothermal process:

$$\frac{\partial}{\partial x}\left(ph^3 Q_{pr} \frac{\partial p}{\partial x}\right) + \frac{\partial}{\partial y}\left(ph^3 Q_{pr} \frac{\partial p}{\partial y}\right) = 12h \frac{\partial}{\partial t}(ph)$$

$$Q_{pr} = 1 + 9.638\left(\frac{P_A}{p}\frac{l}{h}\right)^{1.159}$$

Here, p denotes the pressure, h the gap height, P_A the ambient pressure and h the viscosity. Q_{pr} is a correction term introducing an effective viscosity related to the 'slip', which is occurring for high Knudsen numbers. The cartesian coordinates x and y refer to the planes parallel to the gap.

Hung et al. showed Reynold's equation can be reduced by applying the Galerkin method in combination with an orthogonal basis set of pressure distributions [5]. To be able to perform the necessary integration, Reynold's equation is fully linearized with respect to the pressure p and the gap height h at a given pressure $p_0(x,y)$ and height $h_0(x,y)$. After integration we get as reduced model equation:

$$\underline{\mathbf{PDP}}_{red}[h_0]\dot{\underline{\mathbf{p}}}_{\mathbf{v}} = \underline{\mathbf{PH}}_{red}[p_0, h_0]\underline{\mathbf{q}}_{\mathbf{v}} + \underline{\mathbf{PP}}_{red}[p_0, h_0]\underline{\mathbf{p}}_{\mathbf{v}} + \ldots$$
$$\underline{\mathbf{PDH}}_{red}[p_0]\dot{\underline{\mathbf{q}}}_{\mathbf{v}} + \underline{\mathbf{R}}(p_0, h_0)$$

$$p(x, y, \underline{\mathbf{p}}_{\mathbf{v}}) = P_A + [\ldots \quad p_i(x,y) \quad \ldots]\underline{\mathbf{p}}_{\mathbf{v}};\ \ p_0(x,y) = p(x, y, \underline{\mathbf{p}}_{\mathbf{v0}})$$

$$h(x, y, \underline{\mathbf{q}}_{\mathbf{v}}) = d_0 + [\ldots \quad u_{i,z}(x,y) \quad \ldots]\underline{\mathbf{q}}_{\mathbf{v}};\ \ h_0(x,y) = h(x, y, \underline{\mathbf{q}}_{\mathbf{v0}})$$

where $\underline{\mathbf{p}}_{\mathbf{v}}$ are the linear expansion coefficients with respect to the orthogonal basis set of pressure distributions, p_i the i-th pressure distribution, $\underline{\mathbf{q}}_{\mathbf{v}}$ the generalized coordinates, $u_{i,z}$ the z component of the i-th deformation shape, $\underline{\mathbf{p}}_{\mathbf{v0}}$ and $\underline{\mathbf{q}}_{\mathbf{v0}}$ the 'amplitudes' at the linearisation point, d_0 the initial gap separation and $\underline{\mathbf{PDP}}$, $\underline{\mathbf{PH}}$, $\underline{\mathbf{PP}}$, $\underline{\mathbf{PDH}}$, $\underline{\mathbf{R}}$ the integrals of the linearized Reynold's equations. The remaining term $\underline{\mathbf{R}}$ account for the fact that the equation is

not necessarily linearized at the initial gap separation d_0 and ambient pressure P_A.

An identical integration can be used for a formulation of finite elements for the squeeze film. For this case, a predefined form function for the pressure distribution is used which is related to node values. This form function has to be of such an order, that the pressure gradient is continuos between neighboring elements. Thus, constant mass flow is ensured. If such a FEM element is formulated or elsewhere available, the reduced Reynold's equation can be obtained by simple matrix multiplications of the node vectors representing the pressure distributions with respect to the FEM system matrices, as it was done in the mechanical case. Non-linearities can be modeled by interpolation analogous to the mechanical case described above.

While coupling with the mechanical structure is already incorporated in Reynold's equation, the action of the gas pressure on the mechanical structure has to be considered. Since energy dissipation occurs in the gas film, the coupling force cannot be obtained as derivative of an energy function. Instead, the generalized force term F_v represents the coupling term in this case:

$$F_v = \iint p \frac{\partial \vec{\mathbf{u}}}{\partial q_v} d\vec{\mathbf{A}} = \iint \vec{\mathbf{u}}_v [\ldots \quad p_i(x,y) \quad \ldots] d\vec{\mathbf{A}} \underline{\mathbf{p}_v} = \underline{\mathbf{WP}}_{red,v} \underline{\mathbf{p}_v}$$

As result of the integration, we get a matrix $\underline{\mathbf{WP}}_{\mathrm{red}}$ for the required coupling term. Obviously, the occurring integration can already be evaluated at FEM level. If a corresponding term is added in the used mechanical FEM element, $\underline{\mathbf{WP}}_{\mathrm{red}}$ is obtained by simple matrix multiplication.

3 CHOICE OF BASIS FUNCTIONS

The construction of the macromodel is completed by the definition of orthogonal basis functions for the pressure and deformation configurations. Various methods have been proposed for obtaining proper basis sets, among others mechanical harmonic mode shapes [10] and FEM data obtained from transient runs [5].

The choice is strongly influenced by the system behavior to be investigated. In the case of Σ/Δ-loops the load conditions on the system are not predictable and, as a consequence, short transient analysis is not significant for the system behavior. Due to the feedback forces, the system operates around a preselected fixed state. Therefore, we find it favorable to choose a finite subset of the eigenmodes of the coupled system linearized at this state, to define the reduced manifold of deformation and pressure configurations. Damping, frequency and deformation information associated with an eigenmode serve then as selection criterion for the modes to be used. Since the eigenmodes of the coupled system differ in shape and eigenfrequency from the ones of the undamped mechanical structure, a more accurate representation of the coupled system can be expected, at least in a predefined frequency range for a given number of modes.

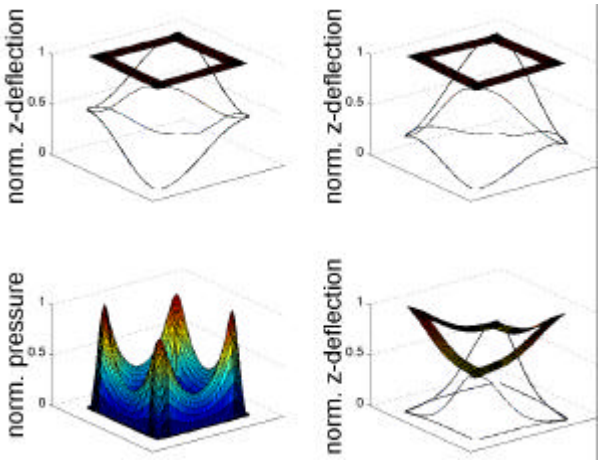

Figure 2: Eigenmodes of the coupled system. *Left*: fundamental mode at $P=10^{-1}$ Pa, *upper right*: distorted mode at $P=10^5$ Pa / -225.1 kHz, *lower right*: distorted mode at $P=10^5$ Pa / -1.8 MHz.

Of course, it is a prerequisite for this procedure, that either a FEM model or an analytical model of the coupled system exists. Furthermore, since the static response of the system requires that the pressure configurations behave independently of those of the mechanical motion, the eigenmodes of the coupled system have to be decomposed into the corresponding parts. Since the consequently obtained basis sets are not orthogonal, their backorthogonalisation is necessary.

If FEM models are available for the coupled problem, the methodology can be automated, since in this case the construction of the macromodel and the choice of the bases is exclusively determined by the meshed FEM model data.

4 TESTSTRUCTURE

As an example we consider the teststructure shown in Fig. 1. To model it, a four-sided, mechanical FEM shell element formulation was extended by the matrices describing the Reynold's equations and the coupling. Here, the Reynold's equations has to be solved in two separate domains formed by the lower and upper gap of the structure. With the eigenmodes of the coupled system, obtained from a modal analysis performed on the FEM model, the macromodel was constructed.

The macromodel has 4 eigenmodes for each set of one deformation and two pressure configurations (one for the upper and one for the lower gap). Using the fundamental deformation and pressure configuration shown in Fig. 2 as complete basis sets, the complex eigenfrquencies of these 4 eigenmodes are listed in Table 1. At low pressure, when damping is negligible, we can expect that the coupled model of the system gives 4 eigenmodes at the same common eigenfrequencies. Table 1 validates this statement. Therefore, the corresponding eigenvectors of the coupled system are composed of the almost identical fundamental pressure and deformation shapes of Fig. 2.

Table 1: Comparison of the eigenfrequencies (E.F.) of the macro model and the coupled FEM model.

model	macro	FEM	macro	FEM
p/Pa	1e-1		1e5	
1 E.F./Hz	-2.0309	-2.0309	-15.7e3	-13.3e3
2 E.F./Hz	-2.0319	-2.0312	-186.5e3	-225.1e3
3 E.F./Hz	-1.4e-4±i*	-4e-3±i*	-1.83e6	-1.80e6
4 E.F./Hz	51.36e3	51.35e3	-2.03e6	-2.03e6

At higher pressure, when damping gets relevant, this relation is no longer valid. Table 1 again lists the eigenfrequencies, which are obtained with the fundamental shapes as complete basis sets for the damped macromodel. The coupled system still has corresponding eigenmodes near these frequencies. The eigenvector at the lowest frequency still matches with the fundamental shapes, but the other ones are distorted due to the damping. Two of these deformation shapes are shown in Fig. 2. Further, their eigenfrequencies shift due to the damping. If these eigenfrequencies still lie in a frequency range, which shall be correctly represented, additional shapes have to be added to the basis sets of the macromodel. With a view to choosing a minimum number of configurations in a specified frequency range, the propre choice are the distorted eigenmodes, selected by means of their eigenfrequencies and mode shapes.

The model of the teststructure, constructed with 4 eigenmodes inserted into the basis sets, was implemented in a system simulator and embedded in the Σ/Δ sense and feedback circuit. Fig. 3 shows the output spectrum of one sense loop at low pressure. Since detection and feedback of the z-component is not orthogonal to one of the higher eigenmodes, this mode is excited. This is indicated by a negative peak in the spectrum. As we have shown elsewhere [7] this kind of excitation can cause the loop to get locked at the corresponding eigenfrequency. Thus, the performance of the signal conditioning is significantly lowered. Similar results were found for this teststructure here, demonstrating, that excitation of eigenmodes can be crucial for the stability of force feedback Σ/Δ-architectures.

5 CONCLUSION

The above results demonstrate that inclusion of damping effects and eigenmodes in macromodels for flexible, squeeze-film damped, micromechanical structures is crucial for the verification of the system performance. The described methodology incorporates these non-idealities and the choice of eigenmodes related to the coupled system ensures correct representation of the dynamical system behavior in a certain frequency range.

By use of appropriate FEM models, the construction of macromodels can be automated by this methodology. The presented coupling scheme can be adapted for other physical domains to extend the region of validity of the macromodels.

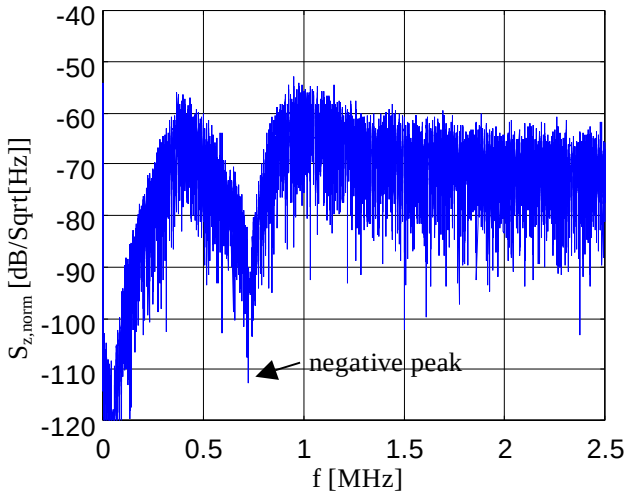

Figure 3: normalized output spectrum for z-axis

REFERENCES

[1] M. Lemkin, B.E. Boser, *A three-axis micromachined accelerometer with a CMOS position-sense interface and digital offset-trim electronics*, IEEE Journal of Solid-State Circuits, vol. 34, no. 4, 1999, pp. 456-68

[2] T. Juneau, A.P. Pisano, *Micromachined Dual Input Axis Angular Rate Sensor*, Solid State Sensor and Actuator Workshop, Hilton Head, SC, USA, June 1996

[3] M. H. Zaman, S. F. Bart, V. L. Rabinovich, C. K. Ghaddar, I. Tchertkov and J. R. Gilbert, *A Technique for Extraction of Macro-Models in System Level Simulation of Inertial Electro-Mechanical Micro-Systems*, Proc. MSM'99, San Juan, Apr. 1999, pp. 163-67

[4] L.D. Gabbay, S.D. Senturia, *Automatic Generation of Dynamic Macro-Models Using Quasi-Statuc Simulations in Combination with Model Analysis*, Solid State and Actuator Workshop, Hilton Head, SC, USA, June 1998, pp. 197-200

[5] E. S. Hung, S.D. Senturia, *Generating Efficient Dynamical Models for Microelectromechanical Systems from a Few Finite-Element Simulation Runs*, IEEE Journal Micromechanical Systems, vol. 8, no. 3, Sept. 99, pp. 280-9

[6] H. Goldstein, *Klassische Mechanik*, 11 Aufl., AULA-Verlag, Wiesbaden, Germany, 1991

[7] M. Handtmann, R. Aigner, F. Plötz, G. Wachutka, *Macromodel for Micromechanical, Multi-Electrode Structures in Force Feedback Control Systems*, Proc. SISPAD'99, Kyoto, Japan, Sep. 1999, pp. 183-186

[8] N.R. Swart, S.F. Bart, M.H. Zaman, M. Mariappan, J.R. Gilbert, D.Murphy, *AutoMM: Automatic Generation of Dynamic Macromodels for MEMS Devices*, MEMS'98, Heidelberg, Germany, 1998, pp. 178-83

[9] T. Veijola, *Finite-Difference Large-Displacement Gas-Film Model*, Transducers 99, Sendai, Japan, 99, 4D1.4

[10] Y. Yang, M. Gretillat, S.D: Senturia, *Effect of Air Damping on the Dynamics of Nonuniform Deformations of Microstructures*, Transducers 97, Chicago, USA, 97, 4A2.1